

Existence of needle crystals in local models of solidification

J. S. Langer

Institute for Theoretical Physics, University of California, Santa Barbara, California 93106

(Received 31 July 1985)

The way in which surface tension acts as a singular perturbation to destroy the continuous family of needle-crystal solutions of the steady-state growth equations is analyzed in detail for two local models of solidification. All calculations are performed in the limit of small surface tension or, equivalently, small velocity. The basic mathematical ideas are introduced in connection with a quasilinear, isotropic version of the geometrical model of Brower *et al.*, in which case the continuous family of solutions disappears completely. The formalism is then applied to a simplified boundary-layer model with an anisotropic kinetic attachment coefficient. In the latter case, the solvability condition for the existence of needle crystals can be satisfied whenever the coefficient of anisotropy is arbitrarily small but nonzero.

I. INTRODUCTION

There is growing evidence that pattern selection in local models of dendritic solidification is closely connected with the existence of so-called "needle-crystal" solutions of the steady-state equations of motion. In both the geometrical^{1,2} and boundary-layer^{3,4} models that have been introduced recently, as well as in more realistic nonlocal models of solidification with diffusion control,⁵ there exists a continuous family of "Ivantsov"^{6,7} needle crystals when surface tension is omitted. The addition of surface tension, however, is a singular perturbation of these systems which, at least in the local versions—that is, the geometrical and boundary-layer models—destroys the family of solutions and opens the possibility that sharp selection of growth rates, tip radii, etc., occurs via a solvability condition. It seems possible that a similar phenomenon occurs in the fully nonlocal problem.

The purpose of the present paper is to examine in some detail the breakdown of the Ivantsov solutions in both of the local models. The way in which this breakdown occurs provides some interesting clues about the roles played by surface tension and crystalline anisotropy in the dendrite theory. Moreover, this singular perturbation problem is of mathematical interest in its own right. As we shall see, the method of solution proposed here seems reasonable but is not rigorous or even systematic. It can, however, be tested by direct numerical computations; and the results of such tests make it plausible that the analytic approximation captures the essential features of the relevant phenomena. Indeed, as this paper is being written, it appears that there may be important new progress both in understanding the mathematical nature of the problem as posed here⁸ and in showing that the basic features of this model problem also appear in the more realistic systems.^{9–11} This paper has therefore been organized to serve as a starting point for study of these later developments.

We shall begin in Sec. II by looking at the simplest nontrivial version of the geometrical model in order to describe the mathematical strategy with a minimum of

unnecessary complication. That strategy will be outlined in Sec. III. In Sec. IV we shall apply this method to a minimal version of the boundary-layer model, and shall see there how crystalline anisotropy may play an essential role in the selection of needle-crystal solutions. Some mathematical and computational details pertaining to both models are relegated to an appendix.

II. THE QUASILINEAR GEOMETRICAL MODEL

In all of the following, we shall restrict our attention to two-dimensional local models in which a moving one-dimensional interface is described by specifying its curvature $K = \partial\theta/\partial s$ as a function of arc length s . The relevant geometry is illustrated in Fig. 1. The basic assumption of the geometrical models^{1,2} is that v_n , the normal velocity of the interface, is a function only of K and its even derivatives with respect to s . The steady-state condition is simply

$$v_n(K, d^2K/ds^2, \dots) = v \cos\theta, \quad (2.1)$$

so that the interface is moving at constant velocity v , without change in its shape, in a fixed direction. A needle crystal, by definition, is a solution of (2.1) that has the general form shown in Fig. 1 in which

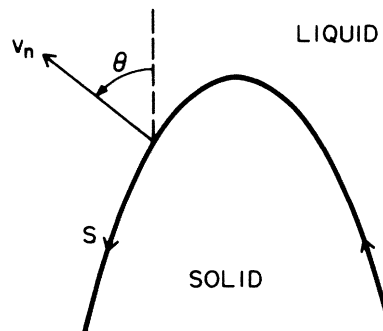


FIG. 1. Geometry of the needle crystal.

$$K \rightarrow 0, \quad \theta \rightarrow \pm \pi/2 \quad \text{as } s \rightarrow \pm \infty. \quad (2.2)$$

The analog of the Ivantsov limit in the geometrical model occurs when we set v_n to be a function of K alone. If (2.1) is piecewise invertible for K as a function of θ , then $K(\theta) = d\theta/ds$ is a first-order ordinary differential equation which generally is solvable for θ as a function of s . We may further expect that these solutions will satisfy the needle-crystal conditions (2.2) for some continuous range of values of the parameter v . For example, the simplest possible choice is $v_n = K$, for which it turns out that

$$\theta = \cos^{-1}(\text{sech } v), \quad (2.3)$$

a relation which satisfies (2.2) for all v . The family of Ivantsov solutions is conventionally characterized by the relation between v and the tip radius $R = K^{-1}(\theta=0)$, which in this case is trivially $Rv = 1$.

The above solutions are all strongly unstable. In fact, the model as it stands is not even dynamically well defined because the amplification rate of deformations is unbounded at short wavelengths. In order to produce a model whose time dependence is meaningful, it is necessary to add a term which mimics the effect of surface tension and stabilizes the system at short wavelengths. The easiest way to do this is to write

$$v_n = K + \gamma^2 \frac{d^2 K}{ds^2}, \quad (2.4)$$

where γ plays the role of a capillary length. Equation (2.4) defines what might be called a quasilinear geometrical model; the right-hand side is linear in K . This model does not actually produce dendrites, but its dynamical behavior is well defined and quite interesting in some respects.

Our aim now is to see what effect the second derivative in (2.4) has on the needle-crystal solutions (2.3). To do this, it is convenient first to rewrite the steady-state equation (2.1) in the form

$$\kappa = \cos \theta - v \frac{d^2 \kappa}{d\xi^2}, \quad (2.5)$$

where $v = (\gamma v)^2$, $K = v\kappa$, and $\xi = vs$. Equivalently,

$$\kappa = \cos \theta - \frac{v}{2} \kappa \frac{d^2 \kappa^2}{d\theta^2}. \quad (2.6)$$

The latter form, in which ξ has been replaced by θ as the independent variable by using $\kappa = d\theta/d\xi$, is very useful but can produce spurious difficulties unless κ is everywhere non-negative.

Equations (2.5) and (2.6) can be used to illustrate some points that have been made in previous papers.^{2,3} If we iterate the right-hand side of (2.6), we generate a series expansion for κ in powers of v and $\cos \theta$. Each term in this series is consistent with the needle-crystal conditions (2.2), and the series appears to produce an accurate estimate for κ especially far down the needle where $\cos \theta$ is small. However, we know that this series can be at best asymptotic. To see this, write (2.5) as a set of three coupled equations for a ξ -dependent trajectory in the space of variables θ , $\kappa = d\theta/d\xi$, and $\lambda = d\kappa/d\xi$. As has been noted previously,² only one trajectory emerges from the fixed

point at $\theta = -\pi/2$, $\kappa = \lambda = 0$; similarly, only one trajectory enters the reflected fixed point at $\theta = +\pi/2$. For a needle crystal to exist, these two pieces must belong to a single trajectory which joins the fixed points and, by symmetry, passes through some point on the κ axis with $\theta = \lambda = 0$. There is no special reason for this to happen. In general, the trajectories entering or leaving the fixed points, even if well approximated by some finite number of terms of the above series in powers of v , need not reach $\theta = 0$ —the tip of the needle—with $\lambda = d\kappa/d\xi = 0$. Our goal in what follows is to compute λ at $\theta = 0$ explicitly and to discover under what conditions it might vanish.

As we shall see immediately, the mathematical problem posed above is highly nontrivial. To make some progress analytically, we shall look only at small values of v ; that is, we shall look in the neighborhood of the known solution of (2.6), $\kappa_0(\theta) = \cos \theta$ at $v = 0$. We then shall consider solutions of (2.6) for nonzero v that satisfy the needle-crystal conditions (2.1) for $\theta \rightarrow +\pi/2$, and shall examine their behavior near $\theta = 0$. This strategy is based on the assumption that, if v is sufficiently small, the difference between κ and κ_0 also will be small in the interval $0 \leq \theta \leq \pi/2$ and may be computable by a linear approximation. For arbitrary v , the continuation of this solution to negative θ may not remain small or even well defined, but the latter behavior need not invalidate an approximation in the region of interest. The trouble with this procedure turns out to be that $\lambda(\theta=0)$ vanishes more rapidly than any finite power of v . Indeed, a systematic expansion in powers of v must necessarily recover just the asymptotic series described above for which $\lambda(0)$ vanishes identically term by term. As a result, any useful scheme of approximation must go beyond a simple series in powers of the small parameter v .

To examine this situation in greater detail, define

$$\kappa - \cos \theta \equiv v\kappa_1, \quad (2.7)$$

and write (2.6) in the form

$$\begin{aligned} v \frac{d^2 \kappa_1}{d\theta^2} - 2v \tan \theta \frac{d\kappa_1}{d\theta} + \frac{1}{\cos^2 \theta} [1 + v(1 - 3 \cos^2 \theta)] \kappa_1 \\ = -\frac{1}{\cos \theta} (1 - 2 \cos^2 \theta) + \mathcal{N}(\kappa_1), \end{aligned} \quad (2.8)$$

where $\mathcal{N}(\kappa_1)$ is a nonlinear term of orders $v^2 \kappa_1^2$ and $v^3 \kappa_1^3$ containing at most two differentiations of these quantities with respect to θ . The structure of (2.8) suggests that each differentiation with respect to θ produces a factor $1/\sqrt{v}$. We shall see this explicitly in what follows. Thus, a systematic approximation for (2.8) might involve dropping \mathcal{N} and the term proportional to v in square brackets on the left-hand side, or perhaps treating these terms perturbatively. The term containing $v d\kappa_1/d\theta$, which is formally of order \sqrt{v} , turns out to be essential. In Sec. III we shall examine the consequences of the above approximation. It will be useful to describe the calculation in general terms so that the technique may be applied to the boundary-layer model in Sec. IV without repetitive explanations.

III. APPROXIMATION SCHEME

The general structure of (2.8), with or without the terms to be omitted, is

$$\nu \frac{d^2 \kappa_1}{d\theta^2} + \nu p(\theta) \frac{d\kappa_1}{d\theta} + q(\theta) \kappa_1 = r(\theta). \quad (3.1)$$

The range of θ is $[0, \pi/2]$. Boundary conditions are to be imposed only at $\theta = \pi/2$. These are the needle-crystal conditions (2.2) which require that κ and $\lambda = d\kappa/d\xi = \kappa d\kappa/d\theta$ vanish as $\xi \rightarrow \infty$, $\theta \rightarrow \pi/2$. If we are working only to first order in κ_1 , then this condition requires that κ_1 and $\kappa_0 d\kappa_1/d\theta$ vanish at $\pi/2$, where κ_0 denotes the Ivantsov solution; that is, $\kappa_0 = \cos\theta$ for the geometrical model. Another way of stating this is that we want κ_1 to be consistent near $\pi/2$ with the asymptotic expansion of κ in powers of ν and $\cos\theta$. To lowest order in ν , this means

$$\kappa_1 \approx r_0(\theta)/q_0(\theta), \quad \theta \rightarrow \pi/2 \quad (3.2)$$

where r_0 and q_0 are the values of r and q at $\nu=0$. Finally, the problem that we pose for ourselves is to compute $\lambda = d\kappa/d\xi$, or simply $d\kappa/d\theta$, at $\theta=0$.

For sufficiently small ν , (3.1) can be solved by a Wentzel-Kramers-Brillouin (WKB) approximation. The homogeneous solutions are

$$\kappa_{\pm}^{\text{hom}}(\theta) \approx \frac{1}{q_0^{1/4}} \exp \left[\pm \frac{i}{\sqrt{\nu}} \psi(\theta) - \frac{1}{2} \int_0^\theta p_0(\phi) d\phi \right], \quad (3.3)$$

where

$$\psi(\theta) = \int_0^\theta q_0^{1/2}(\phi) d\phi, \quad (3.4)$$

and we have neglected terms of order $\sqrt{\nu}$ or smaller in the exponent and in the prefactor. These solutions should be accurate as long as

$$\left| \frac{1}{q_0} \frac{dq_0}{d\theta} \right| \ll \left[\frac{q_0}{\nu} \right]^{1/2}, \quad (3.5)$$

for all θ in $[0, \pi/2]$.

For the quasilinear geometrical model, $q_0 = (\cos\theta)^{-2}$, and (3.5) is satisfied for $\nu \ll 1$. Moreover, $\psi(\theta)$ in (3.4) is equal to the unperturbed dimensionless arc length ξ obtained from $\kappa_0 = d\theta/d\xi = \cos\theta$. Using $p_0 = -2 \tan\theta$, we find

$$\begin{aligned} \kappa_{\pm}^{\text{hom}}(\theta) &\approx \frac{1}{(\cos\theta)^{1/2}} \exp \left[\pm \frac{i}{\sqrt{\nu}} \ln \left[\frac{1 + \sin\theta}{\cos\theta} \right] \right] \\ &= (\cosh\xi)^{1/2} \exp \left[\pm \frac{i\xi}{\sqrt{\nu}} \right]. \end{aligned} \quad (3.6)$$

For small ν , these are rapidly oscillating functions whose amplitudes diverge as $\theta \rightarrow \pi/2$, $\xi \rightarrow \infty$. Equation (3.6) is an analytic statement of the fact that only one trajectory in θ, κ, λ space enters the fixed point at $\theta = \pi/2$, $\kappa = \lambda = 0$, and all other trajectories spiral out and away from that point. It also justifies our expectation that differentiations in (2.8) produce factors of $1/\sqrt{\nu}$.

The next step is to use the homogeneous solutions (3.3)

to compute a particular solution of (3.1) by means of the formula

$$\kappa_1^{\text{part}}(\theta) = \frac{1}{\nu} \int^\theta d\phi \frac{r(\phi)}{W(\phi)} \left[\kappa_+^{\text{hom}}(\theta) \kappa_-^{\text{hom}}(\phi) - \kappa_-^{\text{hom}}(\theta) \kappa_+^{\text{hom}}(\phi) \right], \quad (3.7)$$

where the Wronskian W is

$$W = \kappa_-^{\text{hom}} \frac{d\kappa_+^{\text{hom}}}{d\phi} - \kappa_+^{\text{hom}} \frac{d\kappa_-^{\text{hom}}}{d\phi}. \quad (3.8)$$

The lower limit of integration remains to be chosen. Because both of the homogeneous solutions $\kappa_{\pm}^{\text{hom}}(\theta)$ which appear in (3.7) are inconsistent with the needle-crystal conditions, the only possible choice for this lower limit is $\pi/2$. Using (3.3), we find

$$W(\theta) \approx \frac{2i}{\sqrt{\nu}} \exp \left[- \int_0^\theta p d\phi \right], \quad (3.9)$$

and

$$\begin{aligned} \kappa_1(\theta) &\approx - \frac{1}{\sqrt{\nu}} \int_{\pi/2}^\theta d\phi \frac{r_0(\phi)}{[q_0(\theta)q_0(\phi)]^{1/4}} \\ &\quad \times \exp \left[- \frac{1}{2} \int_\phi^\theta p_0 d\phi' \right] \\ &\quad \times \sin \{ (1/\sqrt{\nu}) [\psi(\theta) - \psi(\phi)] \}. \end{aligned} \quad (3.10)$$

To check that (3.10) does satisfy the asymptotic condition (3.2), integrate (3.10) twice by parts, integrating the sine as if to obtain a series in growing powers of ν . The result is

$$\kappa_1(\theta) \approx \frac{r_0(\theta)}{q_0(\theta)} + \nu M(\theta) + \dots, \quad (3.11)$$

where M is a function of θ which is of no special interest except for the fact that it exists and is well behaved near $\theta = \pi/2$.

Our goal is to calculate $d\kappa/d\theta$ at $\theta=0$, which we denote by the symbol $\kappa'(0)$. Note that the symmetry of the system requires that q and r be even functions of θ and that p be odd. Thus

$$\begin{aligned} \kappa'(0) &= - \frac{1}{2} [q_0(0)]^{1/4} \int_{-\pi/2}^{\pi/2} d\theta \frac{r_0(\theta)}{[q_0(\theta)]^{1/4}} \\ &\quad \times \exp \left[\frac{1}{2} \int_0^\theta p d\phi \right] \\ &\quad \times \cos \left[\frac{\psi(\theta)}{\sqrt{\nu}} \right]. \end{aligned} \quad (3.12)$$

Equation (3.12) is the principal result whose validity and implications are to be explored in the remainder of this paper.

Remember that the condition for existence of a needle crystal is that $\kappa'(0)$ vanish. It is interesting, and possibly useful for future analysis, to note that (3.12) with $\kappa'(0)=0$ can be interpreted as a solvability condition for the (formally) linear inhomogeneous equation (3.1). To see this, consider (3.1) in the whole interval $[-\pi/2, +\pi/2]$ and

look for solutions in the space of symmetric functions $\kappa_1(\theta)$. The function

$$\kappa_{\text{sym}}^{\text{hom}}(\theta) = \frac{1}{q_0^{1/4}} \exp \left[-\frac{1}{2} \int_0^\theta p \, d\phi \right] \cos \left[\frac{\psi(\theta)}{\sqrt{\nu}} \right] \quad (3.13)$$

is the WKB approximation for the solution of $\mathcal{L}\kappa=0$, where \mathcal{L} denotes the linear operator on the left-hand side of (3.1), and

$$\begin{aligned} \tilde{\kappa}_{\text{sym}}^{\text{hom}}(\theta) &= \frac{1}{W(\theta)} \kappa_{\text{sym}}^{\text{hom}}(\theta) \\ &\simeq \frac{2i}{\sqrt{\nu}} \frac{1}{q_0^{1/4}} \exp \left[\frac{1}{2} \int_0^\theta p \, d\phi \right] \cos \left[\frac{\psi(\theta)}{\sqrt{\nu}} \right] \end{aligned} \quad (3.14)$$

is the solution of the adjoint equation $\tilde{\mathcal{L}}\tilde{\kappa}=0$. Thus, the solvability condition derived above has the form

$$\int_{-\pi/2}^{\pi/2} d\theta r(\theta) \tilde{\kappa}_{\text{sym}}^{\text{hom}}(\theta) = 0, \quad (3.15)$$

which is the usual statement that the inhomogeneous term $r(\theta)$ can have no projection onto the null space of \mathcal{L} if (3.1) is to have a solution. One obscure aspect of this interpretation is the definition of the function space; the divergent functions $\kappa^{\text{hom}}(\theta)$ would not seem to belong to the space of acceptable needle-crystal solutions. One can make this difficulty seem less severe by working with the bounded functions $W^{-1/2}\kappa$; that is, by transforming away the first derivative in (3.1). But this mathematical point, among many such points raised in this paper, requires further scrutiny.

The general character of (3.12) can be seen by evaluating it for the quasilinear geometrical model where $q_0 = (\cos\theta)^{-2}$, $p_0 = -2 \tan\theta$, $r_0 = (2 \cos^2\theta - 1)/\cos\theta$, $\psi = \xi$, and $\cos\theta = \text{sech}\xi$. Then, transforming to ξ as the variable of integration, we find

$$\begin{aligned} \kappa'(0) &\simeq -\frac{1}{2} \int_{-\infty}^{\infty} d\xi (\text{sech}^{3/2}\xi) (2 \text{sech}^2\xi - 1) e^{i\xi/\sqrt{\nu}} \\ &\approx -\frac{A}{\nu^{5/4}} \exp \left[-\frac{\pi}{2\sqrt{\nu}} \right], \end{aligned} \quad (3.16)$$

where

$$A = \frac{16\sqrt{\pi}}{15} \simeq 1.8906. \quad (3.17)$$

The derivation of the second form of (3.16), valid in the limit $\nu \ll 1$, is summarized in the Appendix. The important point to notice is that (3.16) has an essential singularity at $\nu=0$, consistent with the failure of expansions in powers of ν .

A comparison between (3.16) and a direct numerical integration of the fully nonlinear equation (2.5) confirms the basic form of (3.16), both the exponential function and the power of ν in the prefactor. The numerically determined value of A , however, appears to be about 3.7 ± 0.2 , larger than that given by (3.17) by a factor of about 2. This comparison was made for values of ν in the interval $0.002 \leq \nu \leq 0.01$, across which $\kappa'(0)$ changes by eight decades. The validity of the asymptotic evaluation of the integral in (3.16) was also checked in this interval by

direct numerical integration, thus confirming that these values of ν are small enough to be in the asymptotic region.

The source of this discrepancy is related to the fact that the power of ν in the prefactor in (3.16), i.e., $\nu^{-5/4}$, is determined by the highest power of $\text{sech}\xi$ in the integrand, which in turn can be traced back to the highest power of $\cos\phi$ in $r_0(\phi)$ in (3.10). (This will be seen explicitly in the Appendix, but should be apparent from (3.16) because there we are computing the high-frequency—small- ν —behavior of a Fourier transform.) Now think about a first nonlinear correction to r . That is, consider using the approximation for κ_1 given in (3.10) to evaluate $\mathcal{N}(\kappa_1)$ and including the result in r on the right-hand side of (3.1). The resulting corrections to r will be formally of relatively high order in ν but will contain various powers of $\cos\theta$, and the latter will produce inverse powers of ν in the final expression for $\kappa'(0)$. The exponential part of (3.16) will be unchanged by this procedure, but apparently the prefactor is not being computed systematically.

This line of analysis will not be pursued further in this paper. It appears that there may be a much more elegant and mathematically controlled way of arriving at formulas such as (3.16).⁸ The interested reader—along with the author—should be alert for new developments in this class of problems.

IV. THE MINIMAL BOUNDARY-LAYER MODEL

The boundary-layer model^{3,4} has been introduced as an attempt to include in a local description some physical features of the real solidification problem that are missing in the purely geometrical approach. In particular, the dynamics of a thermal boundary-layer field defined along the solidification front mimic some of the nonlocality and history dependence associated with a more realistic thermal diffusion field. The model has had some successes. Its steady-state solutions, including the parabolic needle crystal in the Ivantsov limit, are nearly identical to those of the full model. The boundary-layer model does produce time-dependent dendritic patterns whose growth rates and tip radii are numerically consistent with solvability conditions for needle crystals with nonvanishing surface tension. At present, however, it is still not known whether the model produces a physically realistic picture of dendritic sidebranching.

In order to make the following analysis reasonably tractable, we shall consider only a minimal version of the boundary-layer model in which the dimensionless undercooling Δ becomes vanishingly small. This is not the physically most realistic limit of the model, but it retains most of the features which seem essential for present purposes. (The opposite limit, $\Delta \rightarrow 1$, will be discussed elsewhere.) The steady-state equation to be considered is the same as that of Ref. (3), Eq. (5.17), supplemented by an anisotropic kinetic attachment coefficient. Specifically,

$$\kappa = \cos^3\theta - \nu\kappa \cos^2\theta \frac{d}{d\theta} \left[\frac{\kappa}{\cos\theta} \frac{d}{d\theta} (\kappa + b_m \cos\theta) \right], \quad (4.1)$$

where the κ in Ref. 3 has been replaced by $\nu\kappa$ in order to emphasize the analogy to (2.6). Here, $\nu = d_0 v / D \Delta^5$, where d_0 is a capillary length proportional to surface tension, D is the diffusion constant in the liquid, and v is the growth velocity as before. Note that, as in the geometrical model, ν vanishes in the limit of vanishing surface tension and velocity. The quantity b_m in (4.1) is the θ -dependent kinetic coefficient. In the notation of Ref. 4, $b_m = \alpha \Delta^2 (1 - \cos m\theta)$. From here on, we shall specialize to the case $m = 4$, and write $b_4 = 8\beta_4 \cos^2 \theta \sin^2 \theta$.

The Ivantsov limit of (4.1), $\kappa_0(\theta) = \cos^3 \theta$ is a parabola which has unit radius of curvature at its tip and which trivially satisfies the needle-crystal conditions (2.2) for all ν . In analogy to (2.7), let

$$\kappa - \cos^3 \theta \equiv \nu \kappa_1, \quad (4.2)$$

and rewrite (4.1) in terms of κ_1 . The result is an equation of the form (3.1) with

$$p_0(\theta) = -5 \tan \theta + \frac{8\beta_4}{\cos^3 \theta} \frac{d}{d\theta} (\cos^3 \theta \sin^2 \theta), \quad (4.3)$$

$$q_0(\theta) = \frac{1}{\cos^7 \theta}, \quad (4.4)$$

$$r_0(\theta) = 3 \cos \theta (5 \cos^2 - 4) - \frac{8\beta_4}{\cos^2 \theta} \frac{d}{d\theta} \left[\cos^2 \frac{d}{d\theta} (\cos^3 \theta \sin^2 \theta) \right]. \quad (4.5)$$

Inserting these functions into (3.12), we obtain

$$\kappa'(0) \approx -\frac{1}{2} \int_{-\infty}^{\infty} d\psi r_0(\theta) (\cos \theta)^\lambda \times \exp(10\beta_4 \sin^2 \theta) e^{i\psi/\sqrt{\nu}}, \quad (4.6)$$

where $\lambda = \frac{31}{4} + 12\beta_4$ and

$$\psi(\theta) = \int_0^\theta d\phi \frac{1}{\cos^{7/2} \phi}. \quad (4.7)$$

Notice that, in contrast to the geometrical model (3.16), ψ in (4.7) is not quite the same as the unperturbed arc length ξ defined by

$$\xi(\theta) = \int_0^\theta d\phi \frac{1}{\kappa_0(\phi)} = \int_0^\theta d\phi \frac{1}{\cos^3 \phi}. \quad (4.8)$$

The integral on the right-hand side of (4.6) can be evaluated asymptotically in the limit of small ν . Look, for the moment, at the case $\beta_4 = 0$, so that the only integrals needed are Fourier transforms of powers of the function $\cos \theta(\psi)$. An analysis which is outlined in the Appendix yields the estimate

$$\int_{-\infty}^{\infty} d\psi (\cos \theta)^\mu e^{i\psi/\sqrt{\nu}} \approx C(\mu) \nu^{-\alpha} \exp(-a_s/\sqrt{\nu}), \quad (4.9)$$

where

$$a_s = \int_0^1 (1-u^2)^{3/4} du = \frac{3}{5} \sqrt{2/\pi} [\Gamma(\frac{3}{4})]^2 = 0.7189 \dots, \quad (4.10)$$

$$\alpha = \frac{\mu}{7} - \frac{1}{2}, \quad (4.11)$$

and

$$C(\mu) = \left(\frac{2}{7}\right)^{2\mu/7} \frac{2\pi}{\Gamma(2\mu/7)}. \quad (4.12)$$

As in (3.16), the dominant exponential in (4.9) is independent of μ , but the power of ν^{-1} in the prefactor increases with increasing μ . For $\beta_4 = 0$, the leading μ is $\frac{43}{4}$, and

$$\kappa'(0) \approx -\frac{B}{\nu^{29/28}} \exp\left[-\frac{0.7189}{\sqrt{\nu}}\right], \quad (4.13)$$

with

$$B = \frac{15}{2} C\left(\frac{43}{4}\right) \simeq 0.4703. \quad (4.14)$$

Both numerical evaluation of the integral in (4.6) and numerical integration of the fully nonlinear differential equation (4.1) confirm the general form of (4.13). Specifically, a graph of

$$-2\nu^{3/2} \frac{d}{d\nu} \ln[-\kappa'(0)] \approx a - 2\alpha\sqrt{\nu} + \dots \quad (4.15)$$

versus $\sqrt{\nu}$, evaluated for $0.0015 \leq \nu \leq 0.01$ and extrapolated to small $\sqrt{\nu}$, yields $a = 0.71 \pm 0.02 \simeq a_s$ and a value of α of about unity, consistent with $\frac{29}{28}$. A value of B of about 0.8 fits the integration of (4.1), whereas numerical evaluation of the approximation (4.6) confirms (4.14) in giving a value of B of about 0.5. The latter discrepancy is in the same sense and of about the same size as that which occurred for the geometrical model.

The idea that the dominant behavior of $\kappa'(0)$ at small ν is determined by the highest power of $\cos \theta$ in (4.6) provides some interesting information about the effect of crystalline anisotropy. When the anisotropy coefficient β_4 is nonzero, the dominant θ dependence in $r_0(\theta)$ comes from the second term on the right-hand side of (4.5) and enters with the opposite sign. That is, the leading term in $r_0(\theta)$ is proportional to $-\beta_4 \cos^3 \theta$ instead of $+\cos^3 \theta$. As a result, $\kappa'(0)$ must be positive as ν approaches zero. At larger values of ν , however, the exponential factor in (4.6) is no longer oscillating so rapidly, the slower variations in $r_0(\theta)$ make the dominant contributions, and $\kappa'(0)$ becomes negative again. The situation is illustrated in Fig. 2 where $\kappa'(0)$ is drawn as a function of ν for $\beta_4 = 0, 0.1$, and 0.2. These graphs extend out to $\nu = 0.1$, well beyond the asymptotic regime, and have been obtained by integrating the fully nonlinear equation (4.1). Equation (4.6) does seem to remain a qualitatively good approximation as shown by the dashed curves in the figure.

The important point is that, for $\beta_4 \neq 0$, $\kappa'(0)$ vanishes at a finite value of ν , indicating the existence of a steady-state needle crystal. For this particular version of the model, that is, the minimal boundary-layer model ($\Delta \rightarrow 0$) with the special form of kinetic anisotropy indicated in (4.1), such steady-state solutions occur at arbitrarily small but nonzero values of the anisotropy coefficient β_4 . However, the selected value of $\nu = d_0 v / D \Delta^5$ becomes small as β_4 decreases, and it seems highly unlikely that needle crystals with very small v or, equivalently, small d_0 can be stable. Thus, it seems that the minimum value of β_4 required for dendritic behavior in this model is nonzero and is determined by a stability requirement.

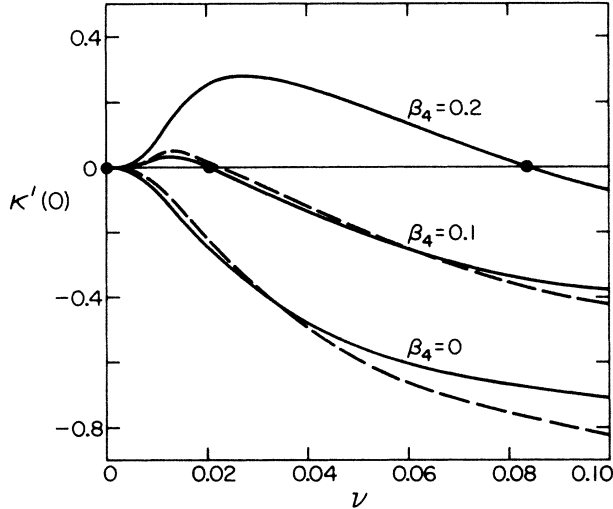


FIG. 2. $\kappa'(0)$ as a function of ν for the boundary-layer model with various values of the anisotropy parameter β_4 . The solid curves have been computed by numerical integration of the nonlinear differential equation (4.1), and the dashed curves by numerical evaluation of the approximation (4.6). The heavy dots indicate values of ν at which the solvability condition is satisfied for the corresponding values of β_4 .

APPENDIX: SOME MATHEMATICAL DETAILS

Asymptotic estimates for $\kappa'(0)$. To derive the asymptotic relation (3.16) for the geometrical model, we must evaluate integrals of the form

$$f_p(\nu) = \int_{-\infty}^{\infty} d\xi (\operatorname{sech}\xi)^p e^{i\xi/\sqrt{\nu}} \quad (\text{A1})$$

in the limit $\nu \rightarrow 0$. This integration is most conveniently carried out by transforming to $\eta = \tan\theta$, where θ is the original angular variable that satisfies $\cos\theta = \operatorname{sech}\xi$. This technique is slightly more cumbersome than necessary for the geometrical model, but turns out to be specially suited for both the boundary-layer model to be considered next and the fully nonlocal problem.¹¹ In terms of η , we have

$$f_p(\nu) = \int_{-\infty}^{\infty} d\eta \frac{1}{(1+\eta^2)^{(1+p)/2}} \exp\left[\frac{i}{\sqrt{\nu}} \psi_G(\eta)\right], \quad (\text{A2})$$

where

$$\psi_G(\eta) = \int_0^\theta d\theta' \frac{1}{\cos\theta'} = \int_0^\eta d\eta_1 \frac{1}{(1+\eta_1^2)^{1/2}}. \quad (\text{A3})$$

Inspection of (A2) and (A3) indicates that we should deform the contour of integration so as to pass near $\eta = i$ and then carry out a steepest-descent calculation in the neighborhood of that point. (The procedure in this case requires that the path of steepest-descent pass through the branch cut and back out again.) If $\eta = i + \omega$, $|\omega| \ll 1$, then

$$\begin{aligned} i\psi_G(\eta) &= i \int_0^i d\eta_1 \frac{1}{(1+\eta_1^2)^{1/2}} + i \int_0^\omega d\omega' \frac{1}{(2i\omega')^{1/2}} \\ &\simeq -\frac{\pi}{2} + (2i\omega)^{1/2}, \end{aligned} \quad (\text{A4})$$

and

$$\begin{aligned} f_p(\nu) &\approx \exp\left[-\frac{\pi}{2\sqrt{\nu}}\right] \int_{-\infty}^{\infty} d\omega \frac{1}{(2i\omega)^{(1+p)/2}} \exp\left[\frac{2i\omega}{\nu}\right]^{1/2} \\ &= \frac{2\pi}{\nu^{(p-1)/2} \Gamma(p)} \exp\left[-\frac{\pi}{2\sqrt{\nu}}\right]. \end{aligned} \quad (\text{A5})$$

Note that, as mentioned previously, the dominant power of ν in the prefactor comes from the largest value of p ; thus, in (3.16),

$$\kappa'(0) \approx -f_{7/2}(\nu). \quad (\text{A6})$$

The same technique works for the integral in (4.9), which we shall denote by $F_\mu(\nu)$. We have

$$F_\mu(\nu) = \int_{-\infty}^{\infty} d\eta \frac{1}{(1+\eta^2)^{(2\mu-3)/4}} \exp\left[\frac{i}{\sqrt{\nu}} \psi_B(\eta)\right], \quad (\text{A7})$$

with

$$\psi_B(\eta) = \int_0^\theta d\theta' \frac{1}{(\cos\theta')^{7/2}} = \int_0^\eta d\eta_1 (1+\eta_1^2)^{3/4}. \quad (\text{A8})$$

Again, writing $\eta = i + \omega$ and integrating along the path of steepest descent through $\eta = i$, we find

$$\begin{aligned} F_\mu(\nu) &\approx \exp\left[-\frac{a_s}{\sqrt{\nu}}\right] \int_{-\infty}^{\infty} d\omega \frac{1}{(2i\omega)^{(2\mu-3)/4}} \\ &\quad \times \exp\left[\frac{2}{7\sqrt{\nu}} (2i\omega)^{7/4}\right], \end{aligned} \quad (\text{A9})$$

which can be evaluated without further approximation to obtain the results shown in Eqs. (4.9)–(4.12).

Numerical methods. Numerical integrations of the nonlinear differential equations (2.5) and (4.1) were carried out with an implicit scheme using θ , κ , and $\lambda = d\kappa/d\xi$ as functions of arc length ξ . Initial conditions were computed using the asymptotic expansions as close to $\theta = \pi/2$ as possible, and then the equations were integrated back to $\theta = 0$. Because, in practice, one can never start precisely on the trajectory which enters the fixed point, there will always be some components of the oscillating homogeneous solutions (3.3) in the function being computed. The frequency of the oscillation in (3.3) provides an estimate of the minimum step size $d\xi$ required to resolve these oscillations accurately. In addition, the rate at which the magnitudes of these homogeneous solutions decay in going toward $\theta = 0$ from $\theta \simeq \pi/2$ provides an estimate of how accurately one must locate the correct trajectory near $\pi/2$ in order to obtain a desired accuracy of the

solution at $\theta=0$. These estimates were confirmed numerically (roughly) and were useful for achieving convergence of the numerical procedure.

Numerical evaluations of the various forms of the solvability formula (3.12), specifically (3.16) and (4.6), were performed using the trapezoidal rule with uniformly spaced intervals in ψ (as if performing a numerical Fourier transform). Results were extrapolated to $d\psi/\sqrt{v} \rightarrow 0$ and tested for convergence in the outer cut-off.

Note added in proof. The connection between singular perturbations and solvability conditions has been discussed by Barenblatt and Zel'dovich^{12,13} in the general context of similarity solutions of partial differential equations. A recent development along these lines, closely related to the work described in the present paper, is the discovery of a solvability condition for pattern selection in

the theory of viscous fingering. An excellent review of the latter topic has been prepared by Bensimon, Kadanoff, Liang, Shraiman, and Tang.¹⁴ I am grateful to L. Kadanoff for informing me about Refs. 12 and 13 and for sending me a copy of Ref. 14 prior to publication.

ACKNOWLEDGMENTS

I should like to acknowledge especially useful conversations about mathematical aspects of this problem with M. Kruskal, C. Oberman, and H. Segur. This research was supported by the U.S. Department of Energy Grant No. DE-FG03-84ER45108, and also in part by the National Science Foundation Grant No. PHY-82-17853 supplemented by funds from the U.S. National Aeronautics and Space Administration.

¹R. Brower, D. Kessler, J. Koplik, and H. Levine, *Phys. Rev. Lett.* **51**, 1111 (1983); *Phys. Rev. A* **29**, 1335 (1984).

²D. Kessler, J. Koplik, and H. Levine, *Phys. Rev. A* **30**, 3161 (1984).

³E. Ben-Jacob, N. D. Goldenfeld, J. S. Langer, G. Schön, *Phys. Rev. Lett.* **51**, 1930 (1983); *Phys. Rev. A* **29**, 330 (1984).

⁴E. Ben-Jacob, N. D. Goldenfeld, B. G. Kotliar, and J. S. Langer, *Phys. Rev. Lett.* **53**, 2110 (1984).

⁵J. S. Langer, *Rev. Mod. Phys.* **52**, 1 (1980).

⁶G. P. Ivantsov, *Dok. Akad. Nauk SSSR* **58**, 567 (1947).

⁷G. Horvay and J. W. Cahn, *Acta Metall.* **9**, 695 (1961).

⁸M. Kruskal, C. Oberman, and H. Segur (private communication).

tion).

⁹D. Meiron (private communication).

¹⁰P. Pelcé and Y. Pomeau (unpublished).

¹¹B. Caroli, C. Caroli, J. S. Langer, and B. Roulet, following paper, *Phys. Rev. A* **33**, 442 (1986).

¹²G. I. Barenblatt and Ya. B. Zel'dovich, *Annu. Rev. Fluid Mech.* **4**, 285 (1972).

¹³G. I. Barenblatt, *Similarity, Self-Similarity, and Intermediate Asymptotics* (Consultant's Bureau, New York, 1979).

¹⁴D. Bensimon, L. P. Kadanoff, S. Liang, B. I. Shraiman, and C. Tang (unpublished).